Influence of Plasma Spray Conditions on the Structure of Al_2O_3 Coatings†

Akira OHMORI*, Chang Jiu LI and Yoshiaki ARATA*****

Abstract

The influence of plasma spray conditions on the structure of Al_2O_3 coatings was quantitatively estimated with three structrural parameters: mean thickness of flattened particles, vertical crack density in the flattened particles and mean bonding rate at the interfaces between flattened particles. All the particles have experienced sufficient flattening to disks of mean lamellar thickness of 1.5 μm to 2 μm, which depends on the velocity, temperature and size of particles.

It is quantitatively illustrated that there exists limited bonding at the interfaces between flattened particles. The maximum mean bonding rate is about 32%. The mean bonding rate is quickly saturated to the maximum when plasma power was increased to 24.5 kW and abrupt drop in mean bonding rate had been observed with the change of spray distance from 100 mm to 150 mm. The coating sprayed with powders of small mean grain size shows a less bonding rate. The mean bonding rate at the interfaces between flattened particles is likely much influenced by the temperature of particles.

It is confirmly shown that vertical cracks occur in all Al_2O_3 coatings with vertical crack density over 1 per 10 μm. The fact that the higher mean bonding rate the higher vertical crack density suggests that the vertical cracks occur during rapid cooling of flattened particles after solidification.

KEY WORDS: (Plasma Spraying) (Alumina Coating) (Structure) (Copper Electroplating) (Flattened Particles) (Mean Lamellar Thickness) (Mean Bonding Rate)

1. Introduction

It is well known that the properties of ceramic materials depend on their structure[1]. It is expected that the properties of thermally sprayed ceramic coating depend also greatly on their structure as that commonly observed for bulk materials. The effective applications of thermally sprayed ceramic coatings to various industrial fields basically rely on good understanding of relationship between properties and structure of the coating, for which an adequate characterization of the structure becomes essential.

Based on the formation mechanism[2], a thermally sprayed coating is deposited through the process that a stream of molten particles with some partially molten particles impact on substrate or formerly deposited coating and flatten laterally, which is followed by rapid solidification. Therefore, the coating has a layer structure markedly different from conventionally processed materials. An individual layer consists of fine-grain structure with meta-stable crystal structure resulted from the rapid cooling[3-4], an intrinsic characteristic of thermal spraying process. In the case of Al_2O_3, the coating mainly consists of meta-stable gamma Al_2O_3 rather than alpha Al_2O_3[3-4], the only stable crystal structure, which was pointed out to be resulted from incompletely melted particles in the spray stream[5]. Furthermore, a thermally sprayed coating inevitably has porosity and pores are different from those in sintered bulk one in structure. The crystal structure of a coating usually can be characterized precisely by *X*-ray diffraction technique. However, the pore structure is much difficult to depict. Up to now, pores are generally characterized based on total porosity in a coating. Recently, porosity is also estimated metallographically from a microstructure of a cross-section of a coating with the aid of image analyzer[6-7], although much ambiguity of pores arises in apparent microstructure resulted from pull-out of particles during sample preparation[8]. With mercury intrusion technique, it was successfully showed that the pores in a coating have a bimode distribution[9-11]. Large pores have size between 1 μm to over 10 μm, but small ones have submicron size between 0.01 μm to 0.4 μm, which are constituted by microcracks in individual lamellae and the imperfect contact between flattened particles[9]. However, as it was pointed out, mercury intrusion method may produce a misleading result because large pores

† Received on November 5, 1990

* Associate Professor
** Graduate Student
*** Emeritus Professor

Transactions of JWRI is published by Welding Research Institute of Osaka University, Ibaraki, Osaka 567, Japan

dominate the total porosity and small pores dominate the distribution of pores[3,11].

On the other hand, the test results for the mechanical properties of coatings, such as tensile test, wear resistance test, erosion test and fracture mechanical test, revealed that the fracture in a coating occurs usually from interfaces between flattened particles[12-15]. This suggests that the interfaces between flattened particles is the weakest part in a coating. The results of fracture mechanical approach suggested that real contact area between flattened particles is much less than the apparent one[15]. The existence of such a non-real contact area was confirmed by direct observation of microstructure of an Al_2O_3 coating by using transmission electron microscope[9]. Comparison of elastic modulus data of a Al_2O_3 coating with sintered one suggested a bonding rate of about 25% between flattened particles[9]. This was also confirmed by a microstructure model for thermal conductivity of ceramic coatings applied to a ZrO_2 coatings compared with that of sintered ceramics[16]. These facts confirmly suggest the important role of interface bonding between flattened particles played in determining the properties of a coating and necessity to estimate quantitatively the interface bonding by proper method rather than only the amount of total porosity. However, no direct measurement of the interface bonding was performed because of the limitation of direct observation. By copper electroplating technique to ceramic coating, by which it has been found that copper can be plated into micro-pores in the coating[17], the structure of an Al_2O_3 coating has been quantitatively characterized by three structural parameters: mean thickness of flattened particles, vertical crack density in flattened particle and mean bonding rate between flattened particles[18]. The results have showed that the limited bonding exists at the interfaces between flattened particles with net-likely distributed vertical microcracks.

Generally, the structure and properties of a certain coating is greatly associated to thermal spray conditions. Therefore, it would be significant to clarify quantitatively the influence of spray conditions on the structure of coating.

Present report describes the effects of plasma power, spray distance, powder feed rate and grain size of powder on the structure of Al_2O_3 coatings quantitatively estimated previously[19] by utilizing copper electroplating method, and discusses the factors influencing coating structure.

2. Materials and Experimental Details

Powder used was commercially available nominally pure Al_2O_3 (Showa-Denko K-16T). The grain size was 10–44 μm and had an average size of about 20 μm. For comparison, powder (Showa-Denko K-17T), which had a grain size of 5–25 μm and mean size of about 10 μm, was also used with an additional indication in the text. The Al_2O_3 coatings were sprayed onto blasted SS41 mild steel surface with Plasmadyne SG-100 spray gun (40 kW). Table 1 shows typical plasma spray conditions. Plasma power and powder feed rate were changed by varying plasma current from 600A to 900A and hopper setting number from 1 RPM to 4RPM (corresponding to powder feed rate of 3 g/min to 12 g/min, respectively) based on the conditions shown in **Table 1**, while the other parameters were kept unvariably. During spraying, the spraying gun was set horizontally and made to traverse mechanically, while the specimen was set vertically and to move up or down vertically to the traverse of the gun at a 5 mm step after the gun had passed through the specimen at a certain spray distance.

The copper electroplating to the sprayed coating was carried out in an alkaline cyanide aqueous solution which was composed of CuCN of 70 g/*l*, NaCN of 90 g/*l* and KOH of 30 g/*l*. A copper rod (10 mm in diameter) was used as an anode, while an Al_2O_3 sprayed sample was used as a cathode. Based on the result of previous study[17], the copper electroplating was carried out with direct current source under cathode current density of 0.5 mA/cm^2 at a temperature of 313 K.

The method to determine the structrural parameters has been given in details in previous papers[18]. Following are brift description of the method. Cross-sections of flattened particles as shown in **Fig. 1** were separated based on the distribution of copper in scanning electron microphotographs of cross-section of a copper electroplated Al_2O_3 coating. Firstly, following

Table 1 Plasma spray conditions

Arc current (A)	800
Arc voltage (V)	35
Plasma gas (*l*/min)	
Argon (primary) at 0.41MPa	57
Helium (auxiliary) at 0.41MPa	28
Powder feed rate (g/min)	4.5
Powder feed gas (*l*/min)	
Argon at 0.55MPa	10.4
Spray distance (mm)	100
Cooling air pressure (MPa)	0.2

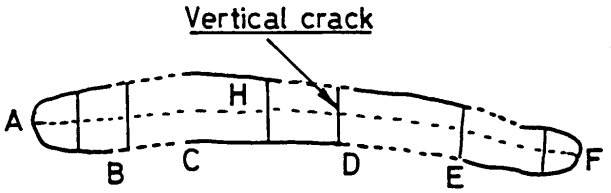

Fig. 1 Schematic diagram of the structure of a cross-section of a flattened particle,: ---- bonded interface; —— nonbonded interface.

parameters were measured directly for individual cross-section of a flattened particle (referring Fig. 1): apparent bonding length (L: ABCDEF); bonded length (l: BC+DE) corresponding to the interface where copper is not recognized; length of a cross-section of a flattened particle (L_1: AHF); area of a cross-section of a flattened particle (S); number of vertical cracks at a cross-section of a flattened particle (N). Then, mean thickness of a flattened particle at a cross-section ($\delta = S/L_1$) and bonding rate (%) ($\alpha = l/Lx100\%$) were calculated. It should be pointed out that the bonding rate here represents the maximum bonding because there might be some isolated pore area which could not be revealed by copper electroplating.

On the basis of the result that mean thickness of flattened particle is independent of apparent bonding length of cross-section, the mean thickness was obtained by calculating mean value of 35 cross-sections of flattened particles at least.

Vertical crack density, expressed in vertical crack number per 10 μm, was obtained from slope of linear relation between vertical crack number and apparent bonding length calculated by using least square fit.

The mean bonding rate was calculated according to following equation.

$$\alpha_m = \sum_i^n l_i / \sum_i^n L_i \quad (1)$$

Where i, n are number of cross-sections of flattened particles.

The relation between α_m and $\sum L$ has shown that when $\sum L$ is larger over 1000 μm, α_m almost approachs a constant. Therefore, α_m was calculated so that $\sum L$ exceeded 1000 μm.

3. Experimental Results

3.1 Effect of spray distance on the structure of Al_2O_3 coatings

Figure 2 shows typical SEM (scanning electron microscope) photographs of Al_2O_3 coatings after electroplated with copper. Al_2O_3 coatings were obtained at 28 kW at different spray distances. When spray distance was increased to 200 mm, it was observed that deposition rate of spray particles decreased largely. Therefore, in order to obtain a coating of about same

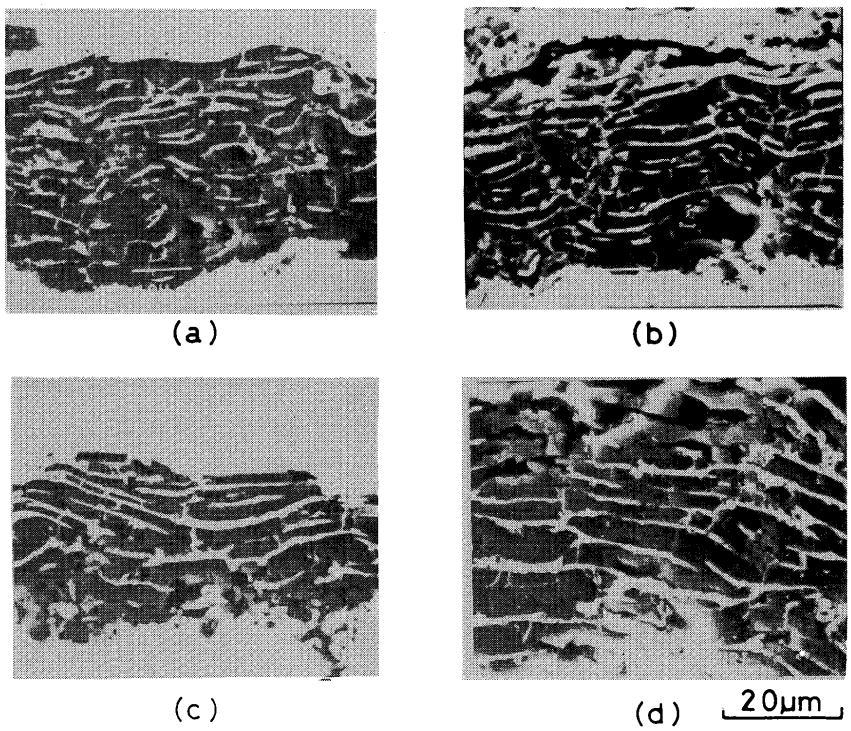

Fig. 2 Micrographs of cross-sections of copper electroplated Al_2O_3 coatings obtained at different spray distances. White parts are copper electroplated into the coatings. (a) 80 mm; (b) 100 mm; (c) 150 mm; (d) 200 mm.

thickness as one at spray distance of 100 mm, overlayer spraying of four passes was performed at spray distance of 200 mm, compared with only one pass in the case of 100 mm. White strings in the microstructure as shown in Fig. 2 represent copper which was electroplated into all kinds of the micro-gaps including pores, micro-cracks, and nonbonded area between flattened particles. The layer structure of the coating became clearly visible by the distribution of copper in a cross-section. Both the vertical cracks in flattened particles and a great deal of nonbonded area between flattened particles could be clearly observed.

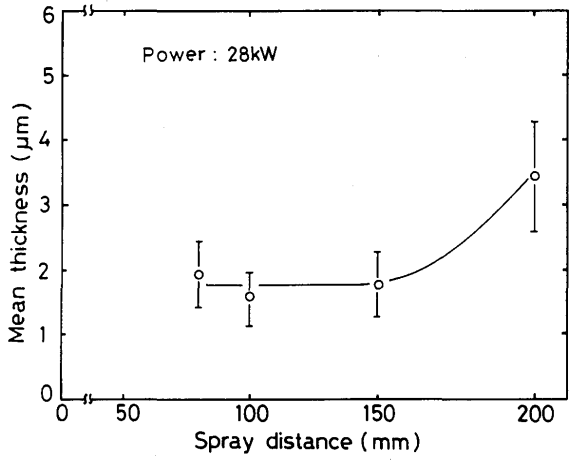

Fig. 3 Effect of spray distance on the mean thickness of the flattened particles in Al_2O_3 coatings.

Figure 3 shows the effect of spray distance on the mean thickness of flattened particles in coatings measured from cross-section of copper plated Al_2O_3 coating. The mean thickness was almost the same and ranged from 1.5 μm to 2 μm until spray distance

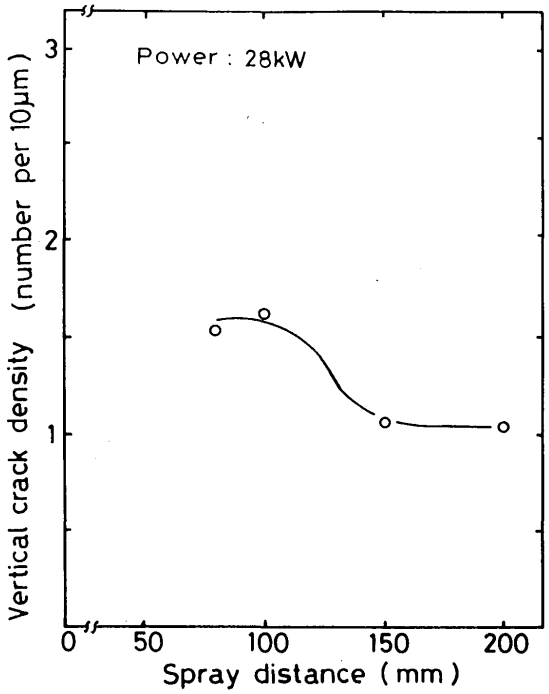

Fig. 4 Effect of spray distance on the vertical crack density in flattened particle in Al_2O_3 coatings.

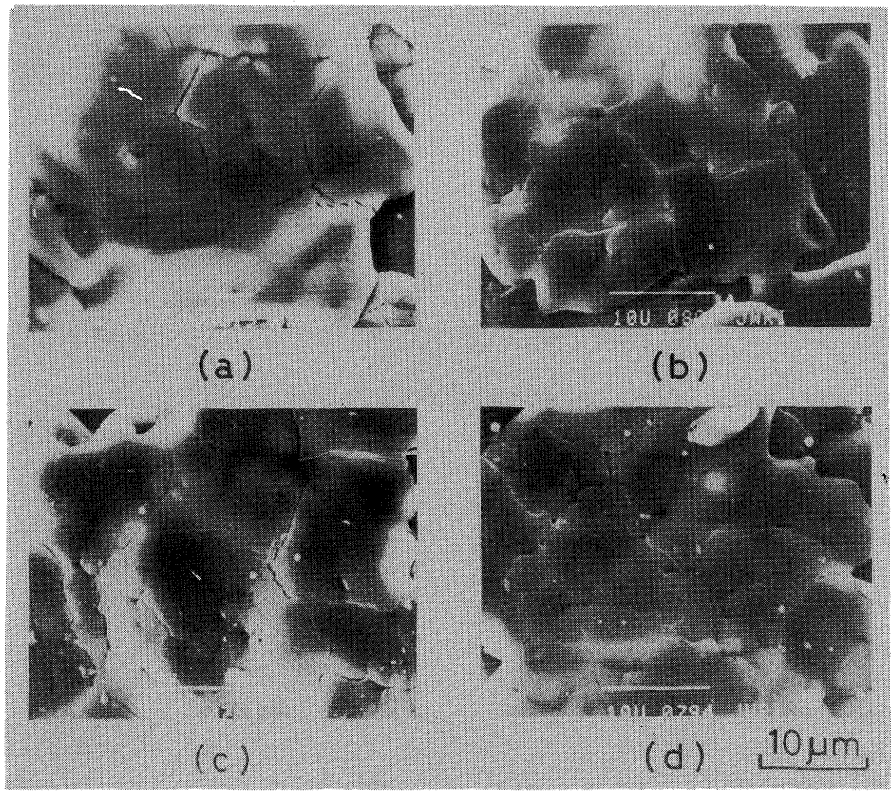

Fig. 5 Surface morphologies of Al_2O_3 coatings obtained at different spray distances. (a) 200 mm; (b) 150 mm; (c) 100 mm; (d) 80 mm.

increased to 150 mm, but it almost doubled to 3.4 μm when spray distance increased to 200 mm.

The effect of spray distance on the vertical crack density in a flattened particle is illustrated in **Fig. 4.** The vertical cracks were observed to penetrate almost one individual layer of flattened particle with homogeneous net-like distribution. The typical surface morphologies of the vertical cracks are illustrated in **Fig. 5** for the coatings sprayed at different spray distance. The mean interval between two adjacent vertical cracks could be approximately estimated from the reciprocal of vertical crack density. As shown in Fig. 4, the vertical crack density was higher until spray distance of 100 mm, while when spray distance increased to 150 mm it became lower. Furthermore, it could be noticed that vertical crack density was larger than 1 per 10 μm. This implied that the mean interval between two adjacent vertical cracks would be less than 10 μm in plasma sprayed Al_2O_3 coatings.

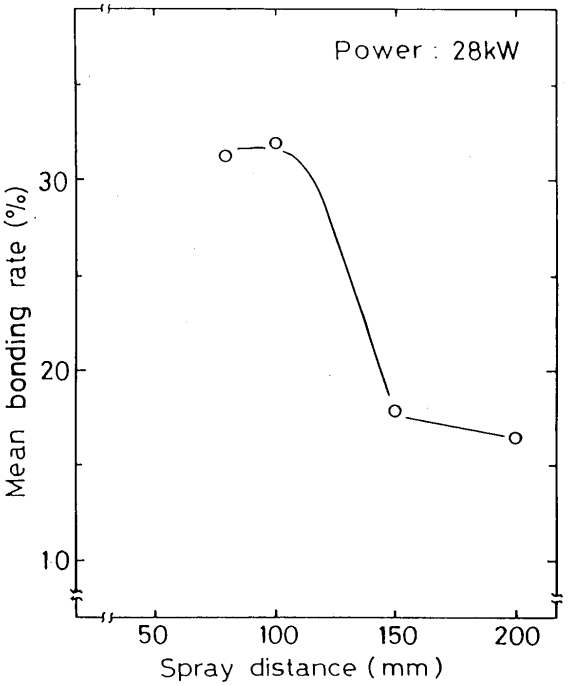

Fig. 6 Effect of spray distance on the mean bonding rate between the flattened particles of Al_2O_3 coatings.

The effect of spray distance on the mean bonding rate is shown in **Fig. 6.** The coatings sprayed at spray distance less than 100 mm had mean bonding rate of about 32%. However, when the spray distance increased further to 150 mm, the mean bonding rate decreased rapidly.

3.2 Effect of the plasma power on the structure of Al_2O_3 coatings

Figure 7 illustrates typical SEM microphotographs of copper plated Al_2O_3 coatings sprayed at different plasma power.

Figure 8 shows the effect of plasma power on the mean thickness of flattened particles. At the spray distance of 100 mm, plasma power showed little

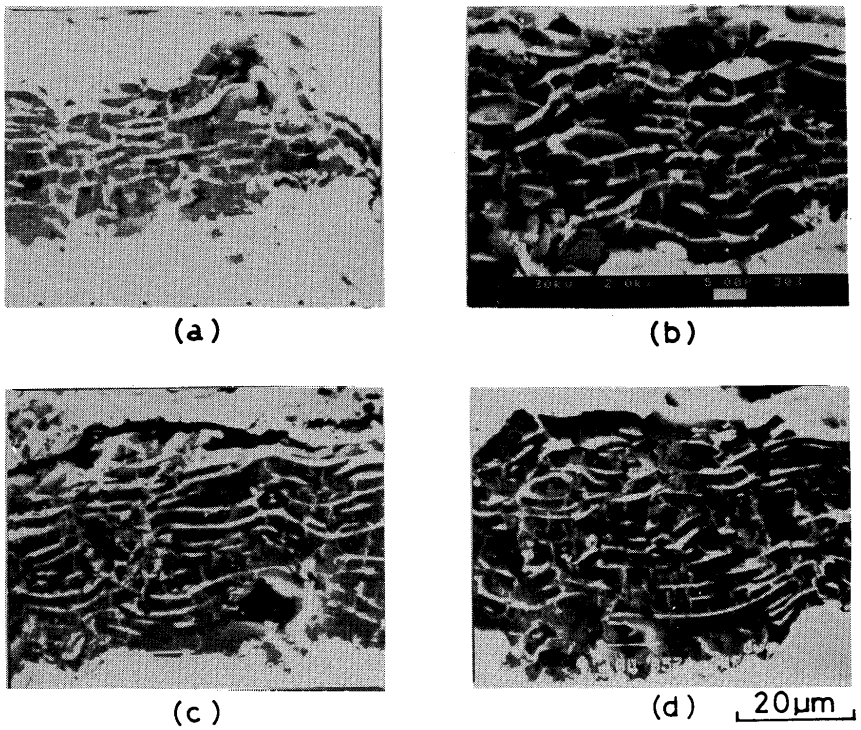

Fig. 7 Micrographs of cross-sections of copper electroplated Al_2O_3 coatings obtained at different plasma powers.
(a) 21 kW; (b) 24.5 kW; (c) 28 kW; (d) 31.5 kW.

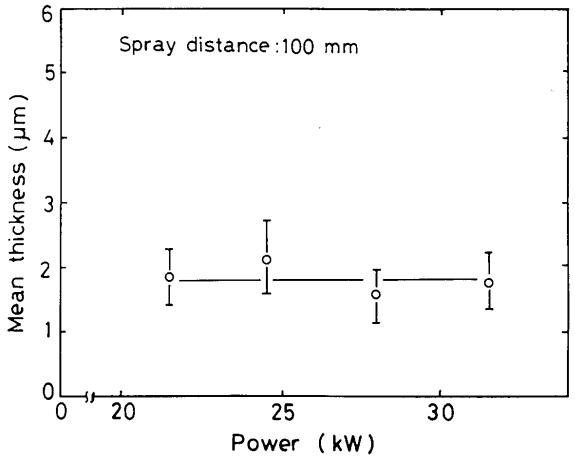

Fig. 8 Effect of plasma power on the mean thickness of the flattened particles in Al_2O_3 coatings.

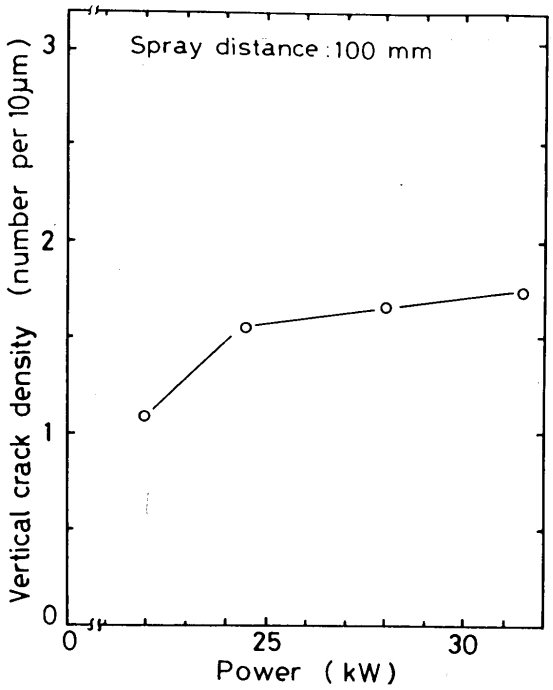

Fig. 9 Effect of plasma power on the vertical crack density in a flattened particle in Al_2O_3 coatings.

influence on mean thickness. All the coatings had the mean thickness from 1.5 μm to 2 μm.

The effect of plasma power on vertical crack density is illustrated in **Fig. 9**. The vertical crack density increased with an increase in plasma power. However, compared with coating obtained at 21 kW, which gave vertical crack density of about 1 per 10 μm, only a little tendency of increase in the vertical crack density was recognized with an increase in power when plasma power exceeded 24.5 kW.

Figure 10 shows the effect of power on mean bonding rate between flattened particles. A lower mean bonding rate was observed for the coating sprayed at

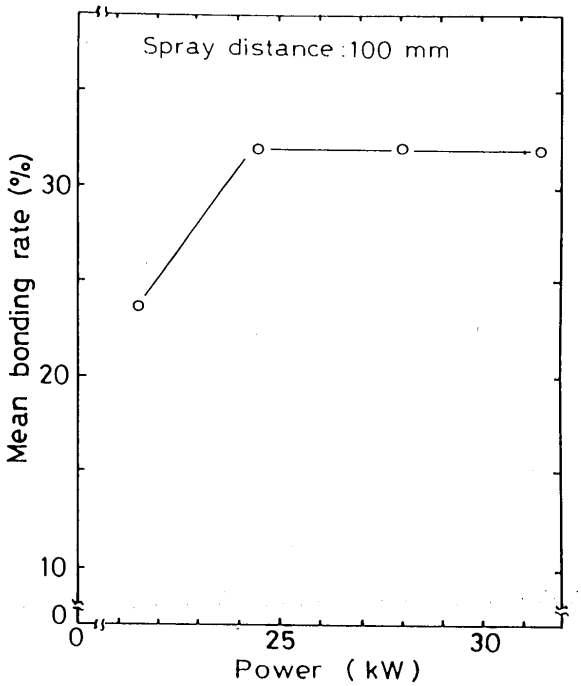

Fig. 10 Effect of plasma power on the mean bonding rate between the flattened particles in Al_2O_3 coatings.

power of 21 kW. When plasma power reached to 24.5 kW the mean bonding rate is saturated to about 32%. No significant increase was recognized with further increase in plasma power.

From above results, it could be also recognized that the vertical crack density in a flattened particle increased with an increase in mean bonding rate at the interfaces between flattened particles.

3.3 Effect of the powder feed rate on the structure of Al_2O_3 coatings

The mean thickness, vertical crack density and mean bonding rate were measured for the coatings sprayed under conditions by only changing powder feed rate from 3 g/min to 12 g/min while the other parameters were kept fixed as shown in Table 1.

Figure 11 gives typical illustrations of microstructure of copper electroplated Al_2O_3 coatings sprayed at different powder feed rate.

The effect of powder feed rate on the mean thickness is shown in **Fig. 12**. All the coatings had mean thickness ranging from 1.5 μm to 2 μm, although a little tendency of increase in mean thickness with an increase in powder feed rate was recognized.

The effects of powder feed rate on the vertical crack density and mean bonding rate are illustrated in **Fig. 13** and **Fig. 14**, respectively. In the extent of present study, until powder feed rate was increased to 12 g/min, no significant effect on the structure of the coatings was recognized.

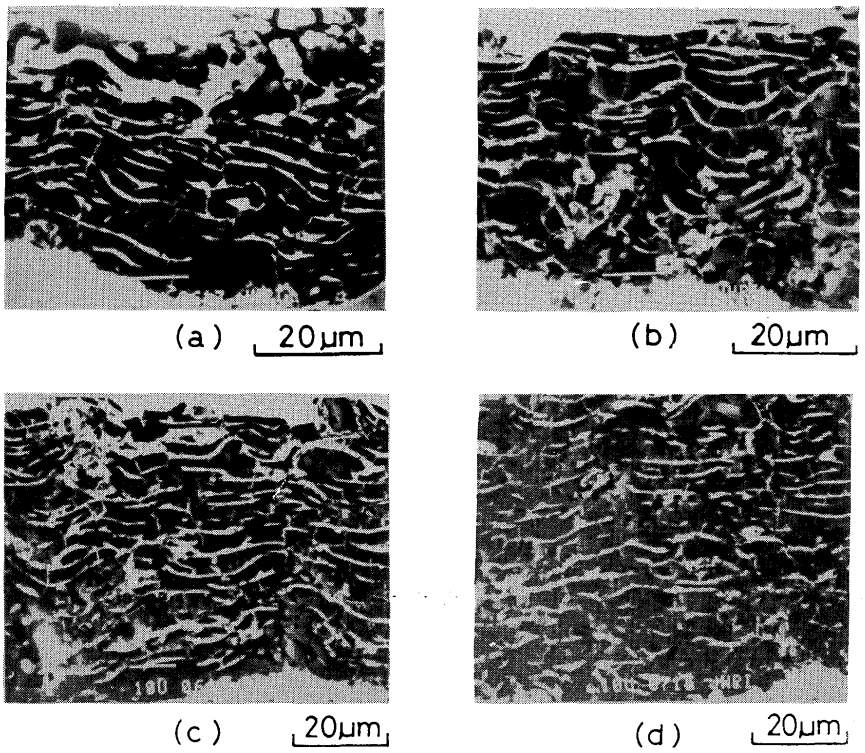

Fig. 11 Micrographs of cross-sections of copper electroplated Al_2O_3 coatings obtained at different powder feed rates.
(a) 3 g/min; (b) 6 g/min; (c) 9 g/min; (d) 12 g/min.

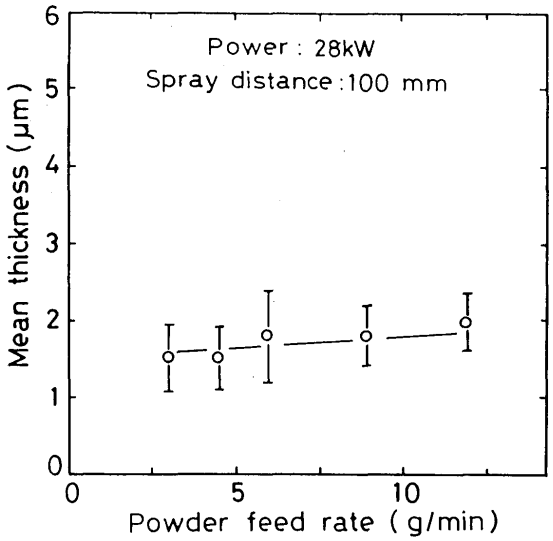

Fig. 12 Effect of powder feed rate on the mean thickness of the flattened particles in Al_2O_3 coatings.

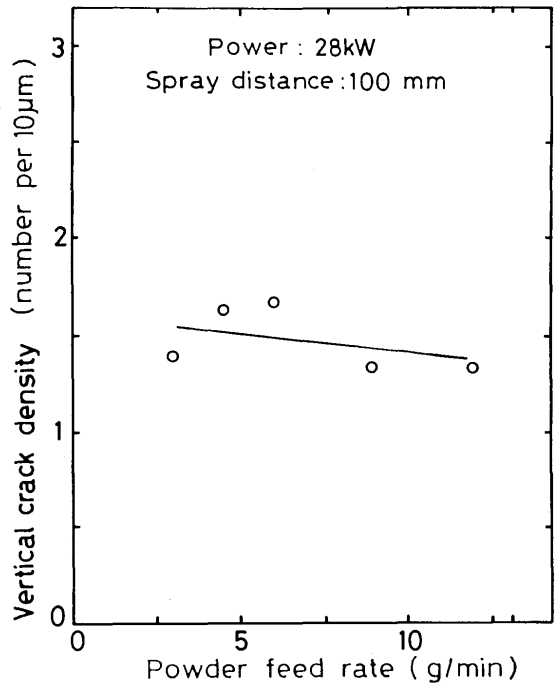

Fig. 13 Effect of powder feed rate on the vertical crack density in flattened particle in Al_2O_3 coatings.

3.4 Effect of the grain size of spray powder on the structure of Al_2O_3 coatings

Figure 15 shows a typical microstructures of the copper plated Al_2O_3 coatings sprayed with the powders of grain size 5-25 μm and mean grain size of 10 μm under spray conditions in Table 1.

Table 2 shows the mean thickness, vertical crack density and mean bonding rate of the coating sprayed with powders which had a mean grain size of 10 μm. The mean thickness and vertical crack density was not significantly different from those of coating sprayed with powders of grain size 20 μm, while mean bonding rate was lower compared with that of the coating sprayed with larger grain size of powder.

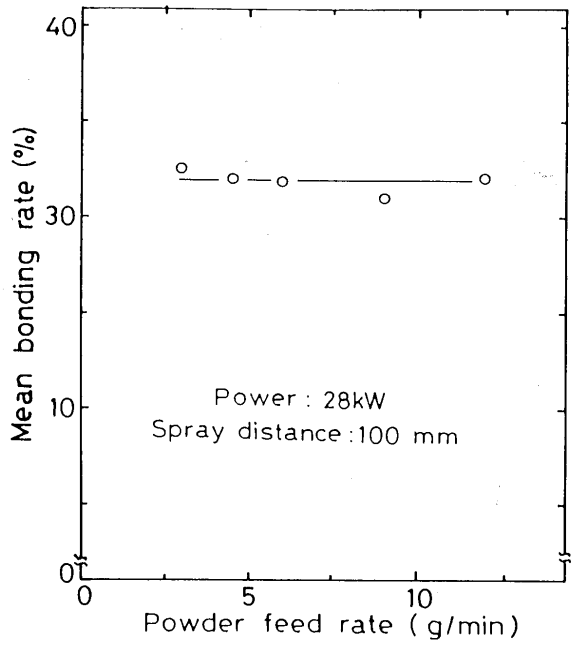

Fig. 14 Effect of powder feed rate on the mean bonding rate between the flattened particles of Al_2O_3 coatings.

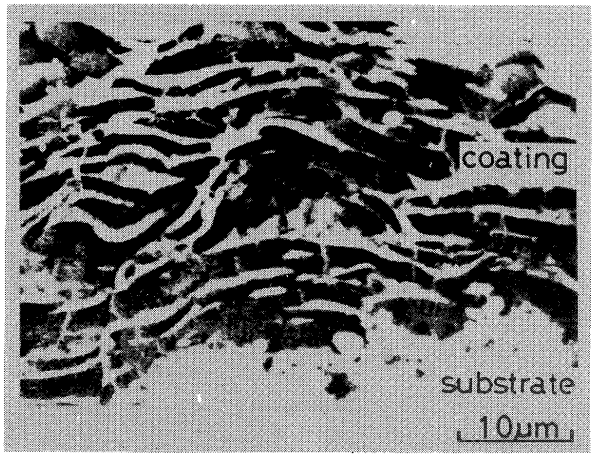

Fig. 15 Micrographs of cross-sections of copper electroplated Al_2O_3 coatings sprayed with powder of grain sizes 5–25 μm.

Table 2 Mean thickness, vertical crack density and mean bonding rate of an Al_2O_3 coating sprayed with powder of 5–25 μm in grain size.

Mean thickness (μm)	1.53±0.36
Vertical crack density (Number per 10 μm)	1.66
Mean bonding rate (%)	19.8

4. Discussion

4.1 The pore structure of thermally sprayed coatings

The microstructure of a thermal sprayed ceramic coating is usually assessed qualitatively from a cross-section of the coating by using optical and scanning electron microscope. The porosity of a coating is also estimated from the microstructure of a cross-section of the coating. From the microstructures of copper electroplated Al_2O_3 coatings, it can be clearly visible that a ceramic coating is deposited with flattened ceramic particles. However, even the lamellar structure can not be usually observed from the microstructure of an as-sprayed coating by optical microscope[18]. Moreover, it is impossible to examine nonbonded interfaces between flattened particles and vertical cracks occurred in individual particle from the microstructure of an as-sprayed ceramic coating. Undoubtly, nonboned area and vertical cracks exist and constitute very important fraction of porosity in a ceramic coating, which is obvious from the microstructure of copper plated Al_2O_3 coating. From the distribution and size of copper deposited into a coating, the dimension of pores can be examined. It can be observed that pores at the interfaces of flattened particles may have size of same order as that of diameter of flattened particle along the direction of flattening although pore channel may be curved when it comes to encounter the bonded area. On the other hand, at the direction perpendicular to flattening pores are very small with submicron size with the exception of pores at the periphery of flattened particles which is of the same size with thickness of flattened particle for Al_2O_3 coatings. The vertical cracks in individual flattened particles appear also like a narrow gaps. The vertical cracks is of submicron size in width but may run to exceed 10 μm. Furthermore, vertical cracks in a ceramic coating also provide much more channels for pores resulted from nonbonded area to be interconnected, which are contributed to total connected open porosity and further responsible for corrosion of the metal substrate in corrosive environment[20] and for oxidation of bond-coating in thermal barrier coating at elevated temperature[21]. Measurement of the pore size distribution for Al_2O_3 coatings by the mercury intrusion method successfully revealed that open porosity has a bimodel distribution[9-10]. Obviously, the size of small pores corresponds to the width of nonbonded area at the interfaces between flattened particles and the width of vertical cracks. On the other hand, large pores would be resulted from insufficient flattening of incompletely melted particles. It was observed that fraction of large pores decreased with spray distance by the mercury intrusion method and small pores showed very little significant change[22]. Therefore, evidently for the optimized ceramic coating, connected pores mainly consist of small ones which are constituted by nonbonded interface area and vertical cracks. However, the limitation of mercury intrusion method is that it is difficult to obtain a true distribution of pores be-

cause the small pores will control the intrusion process of mercury into whole sample[2,11]. Furthermore, it is difficult to distinguish pores rised from nonbonded interface from vertical cracks.

It was observed that there were little large pores in the microstructure of copper plated Al_2O_3 coating which usually appear in the microstructure of as-sprayed one. This fact implies that most of large pores, which usually appear blackly in the microstructure of an as-sprayed ceramic coating during observation, in particular, by optical microscope, possiblly arise from pull-out of particles because of poor bonding between flattened particles and existence of a lot of vertical cracks. Therefore, much care should be taken when attempt is made to assess porosity in a ceramic coating from a microstructure of a cross-section, especially, in quantitative way by using image analyzer.

4.2 Effect of particle temperature and velocity on the mean thickness of flattened particles

The flattening behaviour of a melted droplet when it impacts on a flat surface will be determined by the dissipation of its kinetic energy against viscous flow during spreading of liquid and surface tension. Jones analysed the splat quenching of metals and suggested that the freezing velocity of a splat was orders of magnitude lower than the velocity of flattening so that it is reasonable to considered that flattening of liquid droplet has completed before freezing occurs significantly[23]. By using a model based on the flattening of cylindric liquid between two parallel plates[24], neglecting the effect of surface tension, ratio of droplet diameter (d) to the thickness of flattened particle (δ) can be obtained from following equation.

$$\frac{d}{\delta} = \left(\frac{8\rho dv}{\eta}\right)^{1/4} \qquad (2)$$

where ρ: density of liquid droplet, v: velocity of droplet, η: viscosity of liquid droplet.

Measurements of velocity and temperature for plasma spraying of Al_2O_3 powders with a diameter of 20 μm showed that particles reaches to a velocity of about 200 m/sec and significant proportion of particles reach to a maximum temperature of 2773K and have a mean temperature near melting point (2323K) in the case that plasma power is larger than 25 kW[25]. The minimum solidification temperature of liquid splat will not be the melting point but the temperature to undercooling for homogeneous nucleation ($\simeq 0.8T_m$) which is about 1873K for Al_2O_3[5]. Therefore, the viscosity of liquid droplet may vary from 0.015 Ns/m^2 (at 2773K) to 0.5 Ns/m^2 (at 1873K) with a most proper value of 0.05 Ns/m^2 for particles near the melting point (2323K). Using $\rho = 3.05$ gm/cm^3, $v = 200$ m/sec for Al_2O_3 particle of mean diameter of 20 μm, d/δ is estmated to be 9 and 6.6 at temperature of 2773K and 2323K from equation 2, respectively. From the mean thickness of flattened particles obtained in present study and mean particle size, d/δ yielded value of 10–13 for Al_2O_3 coatings with the exception of the coating sprayed at 200 mm. This gives a reasonable agreement with above calculated value. Calculation from the measured mean thickness gives a value of 2.58 to 3 for the ratio of diameter of flattened disc to that of powder. This gives a good agreement with that measured for isolated particles which gave a value of 2.5–3.5[25]. These facts support confirmly that flattening and solidification of liquid droplet after impacting on a substrate can be considered as two independent processes. For the coating sprayed at 200 mm, if supposing that velocity of particles drops to about 130 m/sec based on reported data[25-26] and the temperature of droplet drops between melting point and homogeneous neucleation temperature, d/δ yields 3.4 to 6.6 from equation 2. This is comparable with observed value of 5.6.

The above mentioned results suggest that flattening of liqiud droplet can be reasonably estimated from equation 2. It is obvious that the effect of plasma spraying conditions on behaviour of flattening of a melted particle will work through such parameters as temperature (viscosity), velocity and size of droplet for a certain materials in a way expressed by equation 2.

4.3 The bonding at the interfaces between flattened ceramic particles

The effect of spray conditions on the mean bonding rate revealed that the mean bonding rate at interfaces between flattened particles in plasma sprayed coatings varied in a range from 16% to 32% under present experimental conditions. The mean bonding rate increased with increase in plasma power at lower power level and saturated rapidly. According to the influence of plasma power on the particle temperature and velocity during plasma spraying[25-26], plasma power of about 22 kW is necessary to melt most powders. Increase in plasma power results in an increase in particle velocity but little change in temperature. The effect of increase in power input on particle heating is to increase the number of particles which are completely molten with little change in the mean temperature near melting point. It might be difficult to interpret results obtained in present study based on above results because of the difference of type of spray gun and powder

feed into plasma jet. However, little increase in mean particle temperature with increase in power input is reasonably consistent with the fact that mean bonding rate shows no significant increase with increase in power input. At power of 21 kW, low deposition rate, which could be recognized from the thickness of coating as shown in Fig. 7, may result from insufficient power to melt most powders and low bonding rate may be brought out by low mean temperature of liquid particle. With the further increase of plasma power, plasma jet will become more effective to heat particle. This effect may only compensate the shortening of resident time of particles in plasma jet brought by increase of particle velocity with increase of power. Therefore, further increase in power contribute to melt almost all particles and reach a mean temperature near the melting point. Therefore, the effect of power input on bonding rate of a flattened particle may mainly work through particle temperature.

The investigation of the influence of spray distance on the distribution of mean particle temperature showed that most particles are at melting point from 9 mm to 140 mm and most particles has droped below melting point at 18 mm at 25 kW[25]. When spray distance exceeds 110 mm mean temperature of particles begins to decrease from melting point with increase in spray distance. On the other hand, particle velocity may decrease from about 240 m/sec to 130 m/sec for 20 μm Al_2O_3 particle when the spray distance was increased from 80 mm to 200 mm for plasma jet operated at 24 kW. The abrupt drop of mean bonding rate at 150 mm may also be resulted from the drop of mean particle temperature. It could be observed that deposit efficience was low at spray distance of 150 mm and at 200 mm droped to about one-forth that at 80 mm and 100 mm. All these facts suggest that particle temperature plays a dominant role in determining the bonding between flattened particles.

The powder feed rate has little influence on mean bonding rate at extent of present study. It may imply that heating of particles has little influence on the heating characteristic of plasma jet. It could be speculated that when power feed rate exceeds 25 g/min the bonding may decrease with further increase of powder feed rate at present torch operating conditions based on the correlation between mean bonding rate and ACT-JP value (reciprocal of particle erosion rate) observed for Al_2O_3 coating[19].

Investigation of the particle size of Al_2O_3 powder on surface temperature of particles showed that for 18 μm Al_2O_3 powder surface temperature reached the maximum in the plasma core and decreased with increase in spray distance, and the smaller the particles the faster the surface temperature decreased[27]. The lower bonding rate observed for the coating sprayed with 5–25 μm powder may also be brought out by abrupt drop in particle temperature at spray distance of 100 mm. This fact implies that small particles should be sprayed at a short distance in order to obtain a coating with high bonding rate. Furthermore, it is difficult to spray a coating of high bonding rate with powders of a wide size distribution. Therefore, it is reasonable that the coating sprayed with the powder of wider size distribution, especially, the powders containing a great amount of small particles in the powders, gave a lower fracture toughness than that sprayed with the powders containing little small particles in the powders[28].

The poor bonding between flattened particles was considered to likely arise from the absorbed or entrapped gases[2]. On the contact between two solid bodys, it was found that adhesion developed between two indium surfaces in the impact experiment (about 2 msec impact) is less than one-third that observed, for an apparent equal area of contact, in a static test (pressed togather for two minutes[29]. This implies that the real contact area in the impact condition would be less than one-third apparent one. It is also pointed out that such a difference is unlikely due to air trapped between the colliding surfaces because experiments carried out in vacuum. It was suggested that the adhesion depends on the time of contact. Generally, when a liquid material is put onto the surface of a solid body which can be wetted each other, it is observed that the contact angle decreases with time, which happens more fastly with the increase in temperature of liquid or solid[30]. During thermal spraying, it can be estimated that the time from impact of droplet to complete solidification may be less than miliseconds based on the facts observed for splat cooling[5,31]. The contact time between flattened liquid and formerly formed cold coating surface is too short for liquid to wet sufficiently identical solid material at rather low temterature. That is, the dynamic process itself as well would play important role during thermal spraying as well. Therefore, low temperature of formerly deposited coating and short contact time would be much responsible to the low bonding between flattened particles.

All the experimental results on the properties of coatings showed that the properties of a coating is much lower than same bulk materials. Investigations on the effect of thermal spraying conditions on the mechanical properties such as microhardness, erosion resistance and tensile strength of coatings revealed that properties of coatings are saturated at a lower level compared

with the bulk materials[23-33]. The tendence is consistent with change of low bonding rate with spray conditions obtained in present study. It has been observed that even for the coatings which have much different apparent porosity, fracture toughness of coatings showed little significant change[34]. It has also been suggested that low elastic modulus of a coating compared with that of sintered material was resulted from low bonding between flattened particles[9]. The microstructure model for ceramic coating which McPherson used to calculate thermal conductivity of a coating confirms the dependence of thermal conductivity of a coating on the bonding rate between flattened particles[16]. All those facts imply that the coating properties, not only mechanical properties, but also thermal and even electric properties are dependent on the bonding between flattened particles.

4.4 Vertical crack in individual flattered particles

It was observed from the distribution of copper electroplated in Al_2O_3 coatings, the penetration of vertical cracks is almost limited in one flattened particle from one surface to the other and the cracks are distributed homogeneously in the form of a net-like which gave mean interval of less than 10 μm between two adjacent cracks. The fact that vertical crack density increases with mean bonding rate confirms that the vertical cracks in flattened particle occurs during cooling of flattened particle after solidification, because thermal contraction is restrained owing to the existence of bonding between flattened particles[18].

The investigation of effect of spray conditions on vertical crack density showed that vertical cracks occurs inevitably in the ceramic coating. Those vertical cracks will provide more channels for pores to be interconnected each other and lead to more connected porosity from coating surface to the interface between substrate and coating.

5. Conclusions

The effect of plasma spray conditions such as plasma power, spray distance, powder feed rate and grain size of powder on the structure of Al_2O_3 coatings was quantitatively estimated by using copper electroplating to the coatings. Three structural parameters used are mean thickness of flattened particles, vertical crack density in the flattened particles and mean bonding rate at the interfaces between flattened particles. The main results can be concluded as follows.

1) The mean thickness of flattened particles in all Al_2O_3 coatings is between 1.5 μm–2 μm except of the coatings sprayed at spray distance of 200 mm, which is unsensitive to spray conditions. The mean thickness depends on velocity, temperature and size of particles.
2) It is quantitatively illustrated that there exists a limited bonding at the interfaces between flattened particles. The maximum mean bonding rate is about 32%. The mean bonding rate is quickly saturated to the maximum when plasma power increased to 24.5 kW and abrupt drop in mean bonding rate has been observed for the change of spray distance from 100 mm to 150 mm. The coating sprayed with powder of small mean grain size shows a less bonding rate. The mean bonding rate at the interfaces between flattened particles is likely much influenced by the temperature of particles.
3) It is confirmed that vertical cracks occurs in all Al_2O_3 coatings with vertical crack density over 1 per 10 μm. The fact that the higher mean bonding rate the higher vertical crack density suggests that the vertical cracks occur during rapid cooling of flattened particles after solidification.

References

1) W.D. Kingery, H.K. Bowen and D.R. Uhlmann; Introduction to ceramics, A Wiley-Interscience Publication, 1976.
2) R. McPherson; The relationship between the mechanism of formation, microstructure and properties of plasma sprayed coating, Thin Solid Films, 83 (1981) 297.
3) V. Wilms and H. Herman; Plasma spraying of Al_2O_3 and Al_2O_3-Y_2O_3, Thin Solid Films, 39 (1976) 251.
4) R. McPherson; On the formation of metastable phase in flame and plasma-prepared alumina, J. Mater. Sci., 8 (1973) 851.
5) R. McPherson; On the formation of thermally sprayed alumina coating, J. Mater. Sci., 15 (1980) 3141.
6) H.-D. Steffens and Fischer; Correlation between microstructure and physical properties of plasma sprayed Zirconia coating, Proc. 2nd National Thermal Spray Conf., ASM Int., 1989, p. 167.
7) Y. Habara; Study on gas tunnel plasma spraying, Doctorial thesis, Osaka University, 1987.
8) A.R. Nicoll, J. Hochstrasser and B. Meier; Controlling factors in the metallographic methods of coating evaluation, Proc. 12th Inter. Thermal Spray Conf., London, June 4–9, 1989, Weld. Inst. of U.K., 1989, P81–1.
9) R. McPherson and B.V. Shafer; Interlamellar contact within plasma sprayed coating, Thin Solid Films, 97 (1982) 201.
10) S. Uemastu, S. Amada, T. Senda and S. Sato; On pore structure of plasma sprayed films, Proc. ATTAC'88, Inter. Symposium on Ad. Thermal Spraying Technol. and Allied Coatings, Osaka, May 12–14, 1988, High Temp. Soc. of Japn., 1988, p. 379.
11) R. McPherson and P. Cheang; Microstructural analysis of Ni-Al plasma sprayed coatings, Proc. 12th Inter. Thermal Spray Conf., London, June 4–9, 1989, Weld. Inst. of U.K., 1989, P. 17–1.
12) L.W. Crane, C.L. Johnston and D.H. James; Effect of processing parameters on the shear adhesion strength of arc sprayed deposits; Proc. 10th Inter. thermal spraying

conf., Essen, May 2–6, 1983, German Weld. Soc., 1983, p. 46.
13) O. Knotek, R. Elsing and N. Strompen; On the properties of plasma sprayed oxide and metal-oxide coatings; Thin Solid Film, 118 (1984) 457.
14) Y. Arata, A. Ohmori and C.J. Li; Basic studies on the properties of plasma sprayed ceramic coatings; Trans. Japn. Weld. Res. Inst., 12 (1986) 339.
15) C.C. Berndt and R. McPherson; A fracture mechanics approach to the adhesion of flame and plasma sprayed coatings; Proc. 9th Inter. thermal spraying Conf., Hague, May 19–23, 1980, Nederlands Instituut voor Lastechniek, 1980, p. 310.
16) R. McPherson; A model for the thermal conductivity of plasma sprayed ceramic coating; Thin Solid Films, 112 (1984) 89.
17) Y. Arata, A. Ohmori and C.J. Li; Characteristics of metal electroplating to plasma sprayed ceramic coatings; Trans. Japn. Weld. Res. Inst., 16 (1987) 259.
18) A. Ohmori and C.-J. Li; Quantitative characterization of the structure of plasma sprayed alumina coating by using copper electroplating, Thin Solid Films, in publication.
19) Y. arata, A. Ohmori and C.-J. Li; Structure and properties of plasma sprayed alumina coatings; J. High Temp. Soc. Japn.; 14 (1988) 220, (In Japanese)
20) Y. Arata, A. Ohmori, J. Morimoto, T. Kudoh, and K. Kishida; Proc. 10th. Int. Thermal Spraying Conf., Essen, May 2–6, 1983, German Weld. Res. Soc., (1983) 197.
21) J. Nerz, G. Bancke, H. Heman and D.S. Engleby; High temperature testing of plasma sprayed thermal barrier coating, Proc. National Thermal Spray Conf., Sept. 14–17, 1987, Orlando, ASM Inter., 1988, p. 253.
22) Kamioka et al; J. Japn. Thermal Spraying Soc., 24 (1988) 1350.
23) H. Jones; Cooling, freezing and substrate impact of droplet formed by rotary atomization; J. Phys. D (Applied Physics); 4 (1971) 1657.
24) G.J. Dienes and H.F. Klemm; Theory and application of the parallel plate plastometer, J. Appl. Phys., 17 (1946) 458.
25) A. Vardelle, M. Vardelle, R. McPherson and P. Fauchais; Study of the influence of particle temperature and velocity distribution within a plasma jet on coating formation; Proc. 9th Inter. Thermal Spraying Conf., Hague, May 19–23, 1980, Nederlands Instituut voor Lastechniek, 1980, p. 155.
26) M. Vardelle, A. Vardelle, and P. Fauchais; Study of the trajectories and temperatures of powders in a D.C plasma jet -Correlation with alumina sprayed coatings; Proc. 10th Inter. Thermal Spraying Conf., Essen, May 2–6, 1983, German Weld. Res. Soc., 1983, p. 88.
27) P. Fauchais, M. Vardelle, A. Vardelle and J.F. Coudert; Plasma spraying of ceramic particles in argon-hydrogen D.C. plasma jet: modeling and measurement of particles in flight, correlation with thermophysical properties of sprayed layer, Metallurgical Trans. B, 20B (1989) 264.
28) P. Ostojic and R. McPherson; A comparison of double cantilever beam (DCB) and indentation methods for determing critical strain energy release rate of plasma sprayed coatings, Proc. 12th Inter. Thermal Spray Conf., London, June 4–9, 1989, Weld. Inst. of U.K., 1989, p. 9–1.
29) A.W. Crook and W. Hirst; Adhesion of indium under static and dynamic loading, Research, 3 (1950) 432.
30) T. Yamaguchi, K. Harano and K. Yajima; Spreading and reactions of molten metals on and with cemented carbides; In Surfaces and Interfaces in Ceramic and Ceramic-Metal Systems; Ed. J. Pask and A. Evans; 1981; p. 503.
31) H. Jones; Splat cooling and metastable phases, Res. Prog. Phys., 36 (1973) 1425.
32) Y. Arata, A. Ohmori and C.-J. Li; Fundamental properties of the ACT-JP, Proc. National Thermal Spray Conf., Sept. 14–17, 1987, Orlando, U.S.A., ASM, Inter., 1988, p. 79.
33) Y. Arata, A. Ohmori, J. Morimoto and A. Yamaguchi; Influence of processing conditions on the thermal sprayed coating, Trans. Japan. Weld. Res. Inst., 15 (1986) 94.
34) G.N. Heintze and R. McPherson; Microstructure and fracture toughness of plasma sprayed Zirconia coating, 15th Inter. Conf. Met. Coatings, San Diego, (1988)